Dynamic Contrast-enhanced MR Imaging Features of the Normal Central Zone of the Prostate

Barry G. Hansford, MD, Ibrahim Karademir, MD, Yahui Peng, PhD, Yulei Jiang, PhD, Gregory Karczmar, PhD, Stephen Thomas, MD, Ambereen Yousuf, MBBS, Tatjana Antic, MD, Scott Eggener, MD, Aytekin Oto, MD

Rationale and Objectives: Evaluate qualitative dynamic contrast-enhanced magnetic resonance imaging (MRI) characteristics of normal central zone based on recently described central zone MRI features.

Materials and Methods: Institutional review board–approved, Health Insurance Portability and Accountability Act compliant study, 59 patients with prostate cancer, histopathology proven to not involve central zone or prostate base, underwent endorectal MRI before prostatectomy. Two readers independently reviewed T2-weighted images and apparent diffusion coefficient (ADC) maps identifying normal central zone based on low signal intensity and location. Next, two readers drew bilateral central zone regions of interest on dynamic contrast-enhanced magnetic resonance images in consensus and independently recorded enhancement curve types as type 1 (progressive), type 2 (plateau), and type 3 (wash-out). Identification rates of normal central zone and enhancement curve type were recorded and compared for each reviewer. The institutional review board waiver was approved and granted 05/2010.

Results: Central zone identified in 92%–93% of patients on T2-weighted images and 78%–88% on ADC maps without significant difference between identification rates ($P = .63$ and $P = .15$ and inter-reader agreement (κ) is 0.64 and 0.29, for T2-weighted images and ADC maps, respectively). All central zones were rated either curve type 1 or curve type 2 by both radiologists. No statistically significant difference between the two radiologists ($P = .19$) and inter-reader agreement was $\kappa = 0.37$.

Conclusions: Normal central zone demonstrates either type 1 (progressive) or type 2 (plateau) enhancement curves on dynamic contrast-enhanced MRI that can be potentially useful to differentiate central zone from prostate cancer that classically demonstrates a type 3 (wash-out) enhancement curve.

Key Words: Prostate cancer; central zone; dynamic contrast-enhanced magnetic resonance imaging.

McNeal's model of prostate anatomy is now over a quarter century old and widely accepted by pathologists, urologists, and radiologists who are involved in the management of prostate cancer (PCa) (1–3). According to McNeal, the prostate can be divided into three glandular zones (peripheral zone [PZ], transition zone [TZ], and central zone [CZ]) and one nonglandular zone (anterior fibromuscular stroma) based on histology, anatomic location, and embryologic features (4). TZ refers to the bilateral regions in the mid to base of the gland, which form two bulges on either side of the urethra that extend superiorly, anteriorly, and laterally from the verumontanum. The CZ is a flattened conical structure located posterior to the TZ and surrounds the ejaculatory ducts (Fig 1). Embryologically, CZ derives from the Wolffian duct whereas TZ is a derivative of the urogenital sinus (5).

The CZ accounts for 25% of the total prostate volume, but almost 40% of the epithelium because of its high epithelial-to-stromal ratio (6,7). It is most prominent at the base of the prostate and has a conical shape, extending inferiorly down to the level of verumontanum and surrounds the ejaculatory ducts (Fig 1). The glands in the CZ are large (about twice the size of those of the PZ) and have irregular contours where epithelial-covered stromal ridges project into the gland lumens (8). McNeal described the epithelial cells of CZ as being columnar, crowded, with somewhat darker granular cytoplasm than those of the PZ (8). CZ glands show unique Roman bridge architecture with the formation of intraglandular lacunae (7,9,10). The secretory profile of CZ glands is also unique and includes cytoplasmic lactoferrin, tissue

Acad Radiol 2014; 21:569–577

From the Department of Radiology, University of Chicago Medicine, 5841 South Maryland Ave, MC2026, Chicago, IL 60637 (B.G.H., I.K., Y.P., Y.J., G.K., S.T., A.Y., A.O.); Department of Pathology (T.A.); and Department of Urology, University of Chicago Medicine, Chicago, IL (S.E.). Received October 21, 2013; accepted January 22, 2014. Disclosure: Neither B.G.H. nor his immediate family members have a financial relationship with a commercial organization that may have a direct or indirect interest in the content. This work was supported in part by the US Army Medical Research and Materiel Command Prostate Cancer Research Program through an Idea Development Award (PC093485). **Address correspondence to:** B.G.H. e-mail: barry.hansford@uchospitals.edu

http://dx.doi.org/10.1016/j.acra.2014.01.013

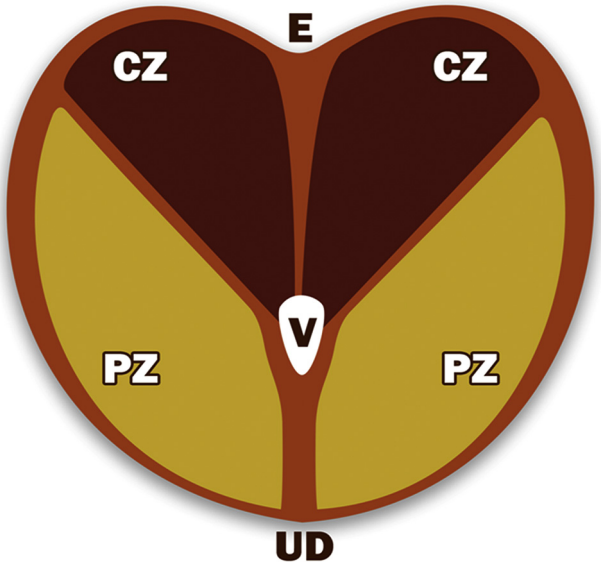

Figure 1. Coronal prostate diagram adapted from McNeal's model of prostate anatomy demonstrating the conical-shaped CZ extending from the base of the prostate to the level of the verumontanum. CZ, central zone; DU, distal urethra; E, ejaculatory duct; PZ, peripheral zone; V = verumontanum.

plasminogen activator, endothelin-1, and numerous lipochrome pigments (7,9,11). With these features, CZ differs from the PZ and TZ and is part way between the features of seminal vesicles and the epithelium of the PZ and TZ (12,13).

Despite these distinct characteristics of the CZ and TZ and data from early anatomic studies indicating that the CZ could be identified distinctly from the TZ on T2-weighted magnetic resonance (MR) images (14,15), many publications in the MR literature have commonly grouped CZ and TZ together as the "central gland" (16,17). Recently, Vargas et al. (18) reported that CZ could be distinguished from other prostate zones in most (81%–84%) patients, based on its location, low signal intensity on T2-weighted images, and apparent diffusion coefficient (ADC) maps. Unfortunately, T2-weighted and diffusion-weighted MR (DW-MR) image features of normal CZ overlap with the features of PCa, and thus CZ can be an important pitfall which mimics PCa, especially at the posterior base, where the prostate is comprised mostly of CZ (18).

As suggested by Vargas et al. (18), one possible means for separating normal CZ from PCa on magnetic resonance imaging (MRI) is dynamic contrast-enhanced (DCE) MRI. The European Society of Urogenital Radiology (ESUR) guidelines for standardized prostate MRI reporting suggest that two functional MRI techniques together with T2-weighted images provide better characterization than T2-weighted images plus one functional technique (19). These guidelines identified DCE-MRI enhancement curve type as a criterion for scoring DCE-MR images in the tabulation of the Prostate Imaging Reporting and Data System (PI-RADS) score indicating the likelihood of significant PCa (19). Unfortunately, as mentioned by Vargas et al. (18), there are no data in the literature about DCE-MRI characteristics of normal CZ.

Thus, the purposes of this study were to determine the detection rate of normal CZ based on the recently described MRI features and to describe the qualitative DCE-MRI characteristics of normal CZ.

MATERIALS AND METHODS

Study Patients

This retrospective study was conducted with an institutional review board–approved waiver of informed consent and was in compliance with the Health Insurance Portability and Accountability Act. We searched clinical records at our institution to identify consecutive patients who underwent preoperative endorectal multiparametric MRI of the prostate between January 2008 and June 2009 who subsequently underwent radical prostatectomy for treatment of PCa. Preoperative multiparametric endorectal MRI (1.5T or 3T) of the prostate was available in 82 patients. An experienced genitourinary (GU) pathologist (7 years of experience in GU pathology) reviewed histologic specimens of the prostate, and 19 patients (23%) were excluded because of either tumor involvement in a portion of the CZ or presence of cancer at the base of the prostate (Fig 2). Of the remaining 63 patients, four were excluded because of DW-MR image artifacts that affected the prostate base. The final study cohort consisted of 59 patients: mean age, 59.9 years; age standard deviation (SD), 7.0; age range, 43–72; average serum prostate-specific antigen (PSA) level, 8.7 mL/ng; PSA SD, 8.0; and PSA range, 1.7–40.9. Of this final cohort of 59 patients, eight whole-mount specimens were evaluated with the GU pathologist to evaluate for concordance of MRI findings of CZ with CZ histology.

MRI Protocols

All MR examinations were performed with an endorectal coil (Medrad, Warrendale, PA) in combination with a phased array surface coil in 1.5T or 3T scanners (33 were performed on 3T, 26 were performed on 1.5T) (Excite HD; GE Healthcare, Waukesha, WI, $n = 33$; Achieva; Philips Healthcare, Eindhoven, The Netherlands, $n = 26$). Immediately before MR examination, 1 mg glucagon (Lilly, Indianapolis, IN) was injected intramuscularly. We imaged the entire prostate and oriented axial images to be perpendicular to the rectal wall guided by sagittal images, and a parallel imaging factor of 2 was used in all sequences. The following axial, coronal, and sagittal images were obtained: T2-weighted fast spin-echo (FSE) (slice thickness 3 mm), axial T1 FSE, axial free-breathing DW imaging ($b = 0$, 1000 and 1500 s/mm^2), and axial free-breathing DCE-MRI. Field of view was 14–18 cm, and resolution was $0.8 \times 0.8 \times 3$ mm. Acquisition of T1-weighted DCE-MRI images (of the entire prostate) started ~30 seconds before intravenous administration of 0.1 mmol/kg gadodiamide (Omniscan; GE Healthcare,